Studies of Sub-Mesoscale Variability of the Ocean Upper Layer Based on Satellite Observations Data

B. Chapron [1, 2, ✉], V. N. Kudryavtsev [2, 3], F. Collard [4], N. Rascle [5], A. A. Kubryakov [3], S. V. Stanichny [3]

[1] *Institute Francais de Recherche pour I'Exploitation de la Mer, Plouzané, France*
[2] *Russian State Hydrometeorological University, Saint-Petersburg, Russian Federation*
[3] *Marine Hydrophysical Institute of RAS, Sevastopol, Russian Federation*
[4] *OceanDataLab, Locmaria-Plouzané, France*
[5] *Centro de Investigación Científica y de Educación Superior de Ensenada, Baja California, México*
✉ bertrand.chapron@ifremer.fr

Purpose. The approach represented in the article is applied to analysis of satellite scanner optical images of high spatial resolution for identifying and quantitative determining the characteristics of the sub-mesoscale dynamic processes in the ocean upper layer.

Methods and Results. The *Envisat AATSR* and *MERIS* SAR-images are used as the satellite data, which permit to determine the ocean surface temperature and surface brightness in the visible range, respectively. Variations in the *s*ea surface glitter contrasts are associated with modulations of the sea surface roughness (rms slope of short waves) on the currents. It is shown that the surface roughness contrasts correlate with the spatial inhomogeneities of the ocean surface temperature, tracing sub-mesoscale processes in the ocean (spiral eddies, filaments, local shears of currents). The described model of formation of surface manifestations is based on interaction between the Ekman current and the main flow vorticity.

Conclusions. Possibility of detecting and quantitative assessing the intense current gradients in the vicinity of sub-mesoscale fronts is shown. These gradients are manifested in the optical satellite images through the ocean surface roughness modulations. The proposed approach makes it possible to study and to assess quantitatively the dynamic processes taking place in the vicinity of the sub-mesoscale fronts. These processes, in their turn, affect the exchange of momentum, heat and gases between the ocean and the atmosphere. The prospects of applying the sub-mesoscale variability defined from the satellite measurements, to development of the models and the systems for the ocean global observations and monitoring are discussed.

Keywords: satellite observations, air-sea interaction, ocean upper layer dynamics, temporal and spatial variability

1. Interactions across spatial-temporal scales

In situ and satellite-based global Earth Observation (EO) systems and platforms have significantly improved our ability to monitor and understand the Earth's environment. The ocean is usually considered as an integrator of the rapidly evolving atmospheric weather noise, resulting in relatively slow ocean variability to evolve on time scales longer than those of the atmosphere. Yet, largely sensitive to ocean

surface changes (sea level, sea surface waves and roughness, foam coverage, current, temperature, salinity and color), satellite measurements often challenge this paradigm to trace and capture spectacular manifestations of fine-scale upper ocean dynamics, including intense fronts and filaments at scales down to less than 100 m.

In certain regions and scales of time and space, these localized ocean-driven processes can then largely dominate the atmosphere variability, to govern upper ocean mixed layer properties. In that context, satellite images obtained with high-resolution satellite sensors, e.g., from passive optical radiometers viewing areas in and around the Sun glitter, provide unique means to monitor the upper ocean. However, outstanding challenges remain to assess the roles of these extreme horizontal and vertical shears that generate these transient processes and features. Consequently, a full quantitative insight of the way how the processes and features influence energy pathways, buoyancy budgets, vertical motions and physical-biology interactions in the upper ocean, and how they structure and concentrate floating material is finally lacking.

To recall, almost all human interactions with the ocean occur in its first few hundred meters in depth. Likewise, most ocean life is concentrated in the upper ocean. As now more clearly recognized, air-sea interaction processes in the upper ocean are essential factors for humanity. Of particular concern, when carbon dioxide is dissolved in water, it produces carbonic acid to alter conditions for marine life. Aforementioned air-sea interactions are also essential factors in determining weather and climate with feedbacks spanning across a very wide time-scale spectrum. This certainly places the upper ocean as an important arena for science transcending the boundaries of physics, chemistry, biology, meteorology and climatology. Yet, no observing- or computer model system can encompass the interacting dynamics of all scales involved in upper ocean dynamics. In particular, computer models can only simulate some of these scales and resulting interactions. Unresolved scales of motion should be parameterized for each type of phenomenon (e.g., surface and internal waves, upwelling and spiraling eddies, ocean surface and currents at depth, vertical velocities, etc.), in terms of its specific effects on the resolved scales.

This largely explains why multi-modal global coverage Earth Observing systems have brought such revolutionary developments to help identify the processes that need to be represented by a sub-grid parameterization at different resolutions. Today, most physical phenomena, or at least their measurable effects, can be observed in data from satellites, drifters and profiling floats. For instance, the observed velocity and the advected quantity data carried by the fluid flow (sea surface temperature, sea surface salinity and chlorophyll, …) represent the synthesis of numerous unknown forcing effects (e.g. effective wind friction including spatial and temporal variations of underlying sea state, surface current, atmosphere stability and upper ocean mixing, …) and related nonlinear interactions, which all are combined to produce the observed state of the flow.

Pushing to higher spatial resolution (about 10 m to 1 km), signatures of tracer variations from imaging instruments can further provide quantitative information, for instance, helping to characterize how internal- and surface waves interact with the ambient underlying upper ocean flow. Foremost, and quite paradoxically, these high-resolution instantaneous snapshots generally produce high-quality data, often revealing an overwhelming wealth of information that can be difficult to fully

decipher and interpret. Frustratingly, the ambition to more precisely approach and understand the impacts of the rapidly fluctuating small-scale components of the upper ocean flow dynamics and structure, has still not been achieved. These ever-growing numbers of very high-resolution satellite observations contribute, unfortunately, to increase the amount of collected and archived data significantly, but yet to be fully exploited.

Thus, while numerous geophysical processes and various oceanic phenomena, developing at very short spatial scales and experiencing rapid fluctuations, are recognized as key contributions to horizontal and vertical fluxes of momentum, heat and tracers, most satellite observations are not fully exploited. Critically, this hampers our ability to fully understand and precisely quantify the role of the smaller scale phenomena, to control the interior ocean dissipation, to interact and shape upper ocean turbulence and to contribute to the emerging coherent structures, eddies and filaments, essential to improve predictions of spatial distributions of lateral eddy fluxes of heat, salt, and other material properties, and/or to contribute to a better understanding of trans-oceanic plastic and species dispersal and marine evolutionary biogeography.

Thus, needs for increased spatial-temporal resolution not only ask for new instrument designs (active and passive technologies, differing frequencies, multi-polarization and viewing angle capabilities, Doppler sensitivity, …), but also call for necessary theoretical developments to refine the use of existing observations with algorithms to consistently interpret the data.

2. Upper Ocean Frontal Dynamics

Fronts commonly sharpen to scales much less than 1 km, and can develop intense current gradients. In that respect, they can be termed as ocean analogues of atmosphere storms and cyclones. Under low wind conditions consecutive of wind-mixing events, sub-mesoscale spirals on the sea [1] are common and manifested in well-organized films of surface active compounds, e.g. organic slicks associated to marine micro-organisms and phytoplankton, Fig. 1. Converging upper ocean flows attract and concentrate naturally occurring surface active material into slicks.
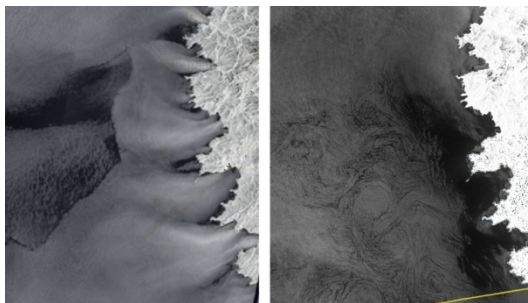
F i g. 1. Evidence of katabatic winds with speed up to 12–15 m/s coming off the west coast of Corsica from the *Sentinel*-1 SAR image on February 19, 2015 (*on the left*); the *Sentinel*-1 SAR image of partially the same region showing manifestations of surfactants and spiraling eddies (*on the right*)

Measurements around sub-mesoscale fronts have already been reported, with current gradients about 1 to 10 f over 500 m. For instance, [2] documented a filament

with cyclonic vorticity of $3f$, f the Coriolis parameter, and convergence of $0.5f$ at 2 km resolution, suggesting gradients larger than $7.5f$ at higher (80 m) resolution. More recently, [3] documented fronts and eddies with convergence/divergence and cyclonic vorticity about 5 to $10f$ over 300 m. [4] described a surprising sharp front, only about 50 m wide despite being elongated over more than 10 km. This leads to current gradients up to $100f$, an order of magnitude larger than previously documented ones.

Local narrow fronts will thus largely escape the geostrophic dynamical balance governing larger eddies, to further develop secondary upper ocean circulation with very large localized vertical velocities. This, in turn, stimulates exchange between surface and deeper ocean [5], and can enhance concentration and transport of surface drifting materials within these convergence areas [6–8]. Those fronts are thus hot spots for biology [9] and drifting pollution [10], including plastics and seaweeds.

With divergence and vorticity values that locally exceed the Coriolis frequency by a factor of 5–50, over a front width of 30 to 100 m [11], oceanic sub-mesoscale ageostrophic processes generally develop with important upwelling mechanism and observed intense local primary production of phytoplankton in the euphotic layer. Large ageostrophic kinetic energy level and surface chlorophyll concentration may thus be often linked. Notably, the resulting detected tracer fine-scale features, are quite systematically observed to correspond to sea surface roughness contrast changes, i.e. locally the surface is glassy or choppy. Indeed, the surface roughness changes, especially the surface wave mean squared slope (*mss*) and/or foam coverage, essentially relate to the modulations of short (wavelength less than ~ 1 m) wind waves by horizontal current gradients [12, 13 and references herein].

As now better understood, different components of the horizontal current gradient can impact different directional properties of the wind-driven, short-scale, sea surface roughness. Specifically, an isotropic divergence of the current has a perfect directional symmetry, resulting in surface roughness anomalies independent on azimuthal view direction. At variance, anisotropic components of the current gradient, like vorticity or strain, can create anisotropic surface roughness anomalies. In such a case, the conditions of detection will be dependent upon the wind direction.

To first help diagnose frontal dynamics, the advective influence of the Ekman transport and diabatic mixing in the Ekman layer must be considered as one of the main mechanisms generating the ageostrophic secondary circulation in the vicinity of oceanic fronts [14, 15]. Considering a local conservation of the vertical vorticity ξ can be considered as a help to interpret upper ocean signatures. Conservation of vertical vorticity writes

$$\frac{d\xi}{dt} \approx -(\xi + f)\nabla u$$

with f, the Coriolis parameter. Convergence or divergence, ∇u, will control the strength of the local shear. This equation also predicts the existence of oscillating linear convergence and divergence zones distributed along the current shear front. For small perturbations, the equation can be approximated as follows

$$\left(u_{\mathrm{Ek}}^x + \frac{\partial \varsigma}{\partial t}\right)\frac{\partial^2 U_y}{\partial x^2} \approx -\left(\frac{\partial U_y}{\partial x} + f\right)\nabla u,$$

with *x, y* the across- and along-front direction, respectively. The shear current is modeled as $U_y(x, y) = U_0 F((x - \varsigma)/L)$, with L the front width, and ς the possibly evolving position of the front. The shape function F may be approximated by a $1 + \tanh(x)$ function. The time-dependent position ς can represent the case of oscillating meanders. To note, this effect can be associated to the process of momentum exchange between the waves and the current (e.g [16]), i.e. the waves pushing outward normal to the flow to alternately increase or decrease the current shear.

Included in the vorticity diagnostic, the across-front ageostrophic Ekman advection, u_{Ek}^x, can also possibly include the Stokes wave contribution, interacting with the surface current. This advection term can also be recognized to enforce and affect local convergence and divergence, ∇u. To note, near fronts, the ageostrophic Ekman spirals will be further modified to take into account the local total upper flow shears. Such local adjustments can thus affect the sign and strength of the resulting divergence fields.

For sharp narrow fronts, the mixing mechanism may also become increasingly efficient, to possibly equal or overcome this advective influence of the Ekman transport [13]. For sake of simplicity to evaluate this overall diabatic mixing effect, we hereafter consider describing the upper flow dynamics with horizontal homogeneous and isotropic turbulence to model upper ocean rapidly-evolving fluctuations. Under this assumption, the slowly-evolving geostrophic balance is simply modified by the horizontal diffusion, and can be hypothesized to simply write

$$f \times u - \frac{a_H}{2} \Delta u = \frac{1}{\rho_b} \nabla p$$

where u is the slow-evolving horizontal velocity, a_H, – a horizontal diffusion coefficient associated to the variance of rapidly-evolving upper ocean fluctuations, ∇p, the slow-evolving component of the pressure, possibly including the additional large-scale wind-stress forcing, and ρ_b is the mean density. For a constant Coriolis frequency f, this equation can be solved in Fourier space. The Helmholtz decomposition of the velocity reads

$$u = \nabla^\perp \psi + \nabla \widetilde{\psi},$$

with

$$\hat{\psi} = (1 + \left\| {\boldsymbol{k}}/{k_c} \right\|^4)^{-1} \frac{\hat{p}}{\rho_b f}$$

where $k_c = \sqrt{2f/a_H}$, corresponds to a spatial cutoff wavenumber, and the hat accent stands for the horizontal Fourier transform. Accordingly, the non-divergent component of the velocity, $\nabla^\perp \psi$, corresponds to the usual geostrophic velocity, weighted by a low-pass filter. For the ageostrophic component of the velocity, $\nabla \widetilde{\psi}$, we have

$$\widetilde{\psi} = \frac{1}{k_c^2} \Delta \psi$$

and this contribution will act to dilate the anticyclones, maximum of pressure and negative vorticity, and to shrink the cyclones, minimum of pressure, and positive vorticity, at small scales. With this development, the divergence of the velocity is proportional to the Laplacian of the vorticity. Naturally, this expression is

reminiscent of the traditional Ekman pumping effect, where divergence and vorticity are related, with a relationship expressed as follows

$$\nabla u = l_{Ek}^2 \partial_z^2 \xi$$

with the vertical vorticity ξ, and l_{Ek} is the thickness of the Ekman layer.

On the other hand, the present development, building on strong stratification and intense horizontal diffusion conditions, isolates the upper ocean dynamics from the interior ones. Indeed, it can be demonstrated that the potential vorticity (PV) becomes zero in the fluid interior [17]. Yet, developments still lead to a slight modification of a standard surface quasi-geostrophic (SQG) model, with the influence of the horizontal diffusion. If the stratification is vertically invariant, N is constant, the modified SQG, expressed in the Fourier space, becomes

$$\hat{b}(\boldsymbol{k}) = N\|\boldsymbol{k}\|\sqrt{1 + \|\boldsymbol{k}/k_c\|^4}\hat{\psi}(\boldsymbol{k})$$

with b stands for the buoyancy, and N the vertical stratification, Brunt-Vaisala frequency. For low wavenumber or moderate horizontal diffusion, $\|\boldsymbol{k}/k_c\|^2 \ll 1$, the standard SQG relationship is recovered. For large wavenumber and/or large horizontal diffusion, near the wavenumber cutoff,

$$\hat{b}(\boldsymbol{k}) = \frac{\sqrt{2}N}{k_c}(\|\boldsymbol{k}\|^2 + \lim_{\|k\|\to k_c}(\|\boldsymbol{k}/k_c\|^2 - 1)^2)\hat{\psi}(\boldsymbol{k})$$

This derivation is still consistent with effective application of the SQG dynamical framework [18, 19]. Here above, the proposed effective filtering applied to SQG derivation appears intermediary between the standard SQG dynamics, with the tracer (buoyancy) proportional to $\|\boldsymbol{k}\|\hat{\psi}(\boldsymbol{k})$, and a purely two-dimensional flow dynamics, with the tracer (vorticity) proportional to $\|\boldsymbol{k}\|^2\hat{\psi}(\boldsymbol{k})$. Nevertheless, contrary to the purely two-dimensional flows or the SQG model, the horizontal velocity is divergent. As derived, the upper ocean vertical velocity, w, is finite and given by the main balance of the buoyancy equation

$$w = \frac{f}{N^2}\frac{\Delta b}{k_c^2}$$

This is consistent with other analytical expressions [14], obtained from considering vertical diffusion and the Omega-equation [20–22]. Here, the horizontal diffusion is emphasized. Under strong stratification and horizontal diffusion, buoyancy anomalies are also strongly linked to vertical motions. Subsequently, an efficient means to diagnose active upper ocean flow dynamics is to consider a high-pass filter, e.g. Laplacian, of the upper ocean buoyancy field.

To summarize, in the vicinity of ocean fronts, both advective influence of the upper flow transport and diabatic mixing must be considered as main mechanisms to generate strong and localized ageostrophic secondary circulation motions. Likely, the local near-surface currents and wave-current interactions will not display classic Ekman wind response characteristics. To first order, the upper ocean wind response will adjust to the ambient flow shear (e.g. [23]). A turbulent thermal (buoyancy) like-wind effect arises [24], possibly including surface wave

induced Stokes impact [25]. Moreover, near fronts, the momentum flux carried by the waves will likely change direction and magnitude. This effect can trigger a reaction force to modify the local shear evolution. This will affect the transport of the upper ocean vertical vorticity of sharp fronts and finally influence the sign and strength of the resulting local divergence field.

3. Sea Surface Roughness Contrasts
to reveal Upper Ocean Frontal Dynamics

For further study of these complex frontal dynamics and to help quantify the different main mechanisms, numerous investigations demonstrate that upper ocean currents can indeed strongly modify the peak wave propagation properties (e.g. [26–28]), but also integral properties of the short wind waves, like the mean squared slope (mss) and wave breaking distribution (e.g. [29–31]).

Fine-scale current gradients at the ocean surface can thus be observed and quantified by analyzing local modulations of peak wave energy and direction, possibly combined with very local sea surface roughness changes. More specifically, directional surface waves and short-scale roughness anomalies can be related to the different horizontal current gradient components [32]. To leading order, the redistribution of swell energy follows the cumulative impact of the large-scale current vorticity field on wave train kinematics. Ultimately, these impacts can lead to significant ray deflection, with the occurrence of focusing/defocusing wave groups in the course of the wave field propagation.

Foremost, very locally, surface roughness modulations are mainly governed by the divergence of the sea surface current field, i.e. ∇u. To first order, the mss contrast, $\tilde{s}$, can be estimated to follow

$$\tilde{s} \propto \frac{m_k}{U_{10}} L_u^{1/2} \nabla u$$

with L_u the spatial extent of the current gradient, and m_k the wave number exponent of the omni-directional spectrum of the short wave action. The roughness contrast is also inversely proportional to the local wind speed, U_{10}. In the present approximation, the propagation of the surface wave energy is neglected. Accordingly, the spatial scale of the surface current L_u must thus be larger than the relaxation scale of the short wind waves, the e-folding time needed by waves to reach back their equilibrium with the local wind. In such a case, the horizontal extension of the roughness frontal width exactly matches the current gradient frontal width. To note, long wave energy, propagating along the wind direction, mostly adjust to surface current over large relaxation distance. Neglecting propagation effects thus mainly favors cross-wind observations to identify and quantify frontal dynamics.

Fig. 2 provides a striking sea surface temperature (SST) exhibiting a very highly dynamical upper ocean in the Gulf Stream area. With high resolution capability O (1 km), this observation is fully adequate to capture mesoscale energetic oceanic signals and sub-mesoscale oceanic features. ENVISAT contemporaneous capability to resolve SST (AATSR instrument) and ocean color (MERIS instrument) helps clearly evidence the link between sea surface roughness changes and frontal SST regions. The field of sea surface roughness contrast, Fig. 3, is derived from the well-resolved Sun glitter brightness sensitivity to local mss variations. When overlaid, Fig. 4, the observed SST, and mss fields provide clear evidence that the synergy approach is

essential for quantitative analysis of the upper ocean dynamics. These combined observations seem to confirm that submesoscale flows are likely energized by mesoscale-driven surface frontogenesis [33–34]. Edges of mesoscale features coincide with sharp surface buoyancy (SST-driven) gradients. Local zooms, Fig. 4 and 5, further illustrate how sea surface roughness contrasts trace anti-cyclonic and cyclonic eddies, fronts and filaments. Following the interpretation framework, alternating contrast changes follow the magnitude and sign of the divergence of the sea surface current field, ∇u.
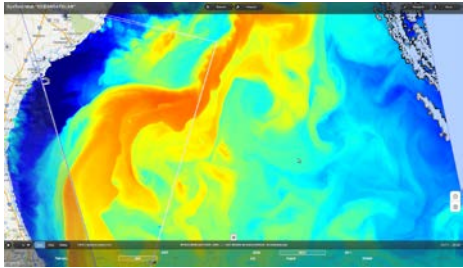
F i g. 2. Sea surface temperature from the *Envisat AATSR* measurements in the Gulf Stream region (April 1, 2010)
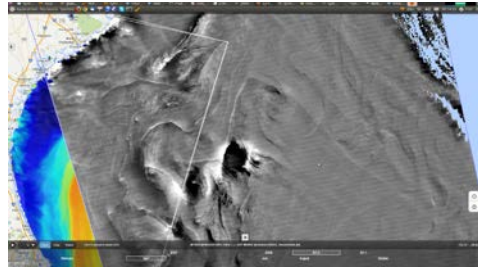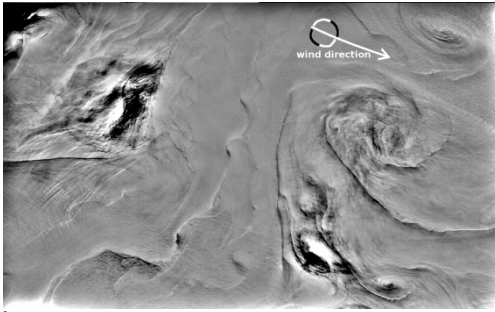

F i g. 3. Sea surface glitter contrasts from the *Envisar MERIS* measurements in the Gulf Stream region (April 1, 2010)
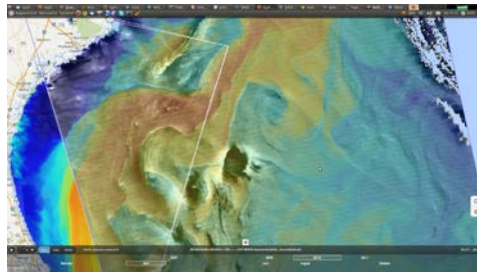

F i g. 4. Overliyng of the simultaneous sea surface temperature (SST) and sea surface glitter contrasts combined from the *Envisat AATSR* and *MERIS* in the Gulf Stream region (April 1, 2010)

Overall, the wind direction relative to the frontal zones also appears to largely prescribed the sign of the divergence, i.e. rough or smooth sea surface areas. More specifically, fronts oriented $\pi/4$ clockwise from the wind direction will be characterized by enhanced rough sea conditions. Fronts, oriented $\pm\pi/4$ clockwise from the wind direction, are quite systematically characterized by smooth sea conditions (Fig. 4 and 5). The favoring $\pi/4$ orientation will need further research. Yet, it can be recalled that wave momentum changes associated with wave amplitude variations are maximum for incoming waves that impinge the front with a $\pi/4$ orientation. A reaction force can then be hypothesized to modify the local shear evolution, to finally influence the sign and strength of the resulting local divergence field.

F i g. 5. Zoom for the sea surface glitter contrast extracted from the *Envisat MERIS* observations in the Gulf Stream region. Wind direction is indicated by the arrow. Bright (dark) contrasts correspond to rough (smooth) sea surface. Sea surface roughness contrasts trace anti-cyclonic and cyclonic eddies, fronts and filaments. The *Envisat MERIS* pixel resolution is 250 m
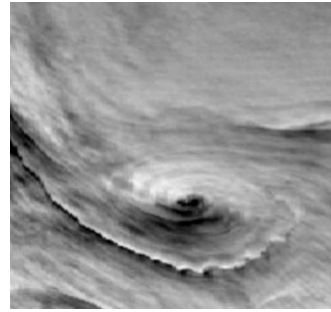
F i g. 6. Zoomed region (the lower right part of Fig. 5) with sea surface glitter contrast identifying the spiraling ocean cyclonic eddy: instabilities are evidenced by the winding outer boundary. The *Envisat MERIS* pixel resolution is 250 m

4. Summary and outlook

A new age of upper ocean observations is now gradually emerging. Large to medium spatial-temporal observing and monitoring technologies that have proved their worth for oceanography and climate science (e.g., satellite altimetry, Argo profilers) have reached maturity for present coupled data assimilation. The next generation of simulation codes will then also face new challenges that are generally largely beyond the capabilities of present deterministic predictions, e.g. dealing with local and intense extreme horizontal and vertical velocity shears, coupled with atmosphere coupled adjustments. Meeting these challenges will require dealing with uncertainty through advanced stochastic modelling and mathematical analysis, applied in concert with high-resolution observations, computational nested simulations, including improved geophysical retrieval algorithms more constrained with sensor physics and analysis of large datasets.

Within the European Copernicus program ensuring a long-term perspective through the Sentinel missions, a new Copernicus Imaging Microwave Imaging Radiometers (CIMR, see [35]) having improved resolution capability has now been accepted. NASA/CNES will launch (in 2022) the Surface Water Ocean Topography (SWOT) mission (see [36]). SWOT will map the ocean surface mesoscale sea surface height field, as well as a large fraction of the associated submesoscale field.

Foremost, a great portion of very-high resolution multi-modal observations, i.e. snapshots, from all other available future imaging sensors (active and passive) must also be considered to be combined in a new regime of medium to high resolution observations of upper ocean dynamics. Upper ocean dynamics is influenced by many factors. This includes variable atmosphere fluxes, rain, river runoff, surface and internal waves, Langmuir circulation, mixing, and biological process. Yet, in reality the observations often bear and integrate the full signatures of all of these complex interacting effects [37]. In particular, a crucial aspect is to better document the local and rapidly fluctuating components of the upper ocean flow velocities.

In that endeavor, sensors operating at very high resolution are essential, especially to successfully locate and estimate sharp current gradients. For practical applications, the precise location of accumulated drifting material can be achieved, and near-real-time availability of ocean surface roughness images may be useful for operational purposes related to pollution or search and rescue operations.

In addition to locate the front very precisely, high resolution sensors can

accurately estimate the current gradient at the front, to monitor areas of current gradient intensification within the different sub-mesoscale features. Under clear-sky conditions, multi-angular optical instruments with 10 m pixel resolution can be ideal to help identify frontal processes that need to be represented by a sub-grid parameterization at different resolutions [28, 38]. Using all-weather high-resolution radar observations, polarization sensitivity [39] and azimuth diversity can be exploited to quantitatively separate the measured roughness variations between changes associated with denser breaking patches and purely resonant short-scale scatter modulations, i.e. to separate effects associated with surface currents and wind variability [40]. Under moderate wind speed conditions, small and intermediate scale breaking waves have relatively small relaxation scale (about 5 to 100 m), to precisely locate the intense surface current variations. Moreover, polarization sensitivity and azimuth diversity also control high-resolution radar Doppler measurements (e.g. [41, 42]) to further document the instantaneous upper ocean flow velocities that cannot be sufficiently resolved at the slow temporal and spatial scales.

In this paper, the analysis strategy to apply to instantaneous high-resolution satellite observations is shown. It demonstrates the possibility to both detecting and quantifying strong current gradients from surface roughness modulations, to help study and quantify the dynamical mechanisms at play around sub-mesoscale fronts, including oceanic, atmospheric or wave-related mechanisms.

These processes, which also impose distinct changes in ocean-atmosphere exchange of momentum, heat and gases, with profound implications on ocean biogeochemistry and climate, are quite systematically revealed in single-time snapshot imaging acquisitions. However, formal methods to bridge instantaneous observations with long-time (past and future) evolutions are still to be defined.

In that context, strategies to blend the information between parameters controlling high-resolution simulations, informed by both low- and high-resolution data (in either space, time or both), merging those derived from multi-modal satellite and in-situ observations must be developed: the next generation of models must be capable of handling full resolution but also not regularly sampled snapshot measurement data sets. To help, the importance of Machine Learning (ML) is quickly advancing to provide new powerful tools to extract information from large amounts of data, i.e. from an ensemble of simulations and accumulated observations. Thus, the significant steps forward will certainly be anticipated by developing and applying these ML methods to maximize the use of multi-modal high-dimensional data. The full characterization of intermittent, multi-scale and transient processes and dynamics using physics informed data-driven analysis certainly remains an open challenge, but will be necessary to provide quantitative insight of how these processes influence energy pathways, buoyancy budgets, vertical motions and physical-biology interactions in the upper ocean.

All data can be accessed from Syntool (www.oceandatalab.com) and from CMEMS (http://marine.copernicus.eu/services-portfolio/access-to products/?option=com_csw&view=details&product_id=MULTIOBS_GLO_PHY_ NRT_015_003).

REFERENCES

1. Munk, W., Armi, L., Fischer, K. and Zachariasen, F., 2000. Spirals on the Sea. *Proceedings of the Royal Society A, Mathematical, Physical and Engineering Sciences*, 456(1997), pp. 1217-1280. https://doi.org/10.1098/rspa.2000.0560

2. Flament, P. and Armi, L., 2000. The Shear, Convergence, and Thermohaline Structure of a Front. *Journal of Physical Oceanography*, 30(1), pp. 51-66. https://doi.org/10.1175/1520-0485(2000)030<0051:TSCATS>2.0.CO;2

3. Ohlmann, J.C., Molemaker, M.J., Baschek, B., Holt, B., Marmorino, G. and Smith, G., 2017. Drifter Observations of Submesoscale Flow Kinematics in the Coastal Ocean. *Geophysical Research Letters*, 44(1), pp. 330-337. doi:10.1002/2016GL071537

4. Rascle, N., Chapron, B., Molemaker, J., Nouguier, F., Ocampo-Torres, F.J., Osuna Cañedo, J.P., Marié, L., Lund, B. and Horstmann, J., 2020. Monitoring Intense Oceanic Fronts Using Sea Surface Roughness: Satellite, Airplane

and In Situ Comparison. *Journal of Geophysical Research: Oceans*, 125(8), e2019JC015704. https://doi.org/10.1029/2019JC015704

5. Lapeyre, G. and Klein, P., 2006. Impact of the Small-Scale Elongated Filaments on the Oceanic Vertical Pump. *Journal of Marine Research*, 64(6), pp. 835-851. https://doi.org/10.1357/002224006779698369

6. D'Asaro, E.A., Shcherbina, A.Y., Klymak, J.M., Molemaker, J., Novelli, G., Guigand, C.M., Haza, A.C., Haus, B.K., Ryan, E.H., [et al.], 2018. Ocean Convergence and the Dispersion of Flotsam. *Proceedings of the National Academy of Sciences*, 115(6), pp. 1162-1167. doi:10.1073/pnas.1718453115

7. Kubryakov, A.A., Aleskerova, A.A., Goryachkin, Yu.N., Stanichny, S.V., Latushkin, A.A. and Fedirko, A.V., 2019. Propagation of the Azov Sea Waters in the Black Sea under Impact of Variable Winds, Geostrophic Currents and Exchange in the Kerch Strait. *Progress in Oceanography*, 176, 102119. doi:10.1016/j.pocean.2019.05.011

8. Aleskerova, A.A., Kubryakov, A.A., Goryachkin, Yu.N., Stanichny, S.V. and Garmashov, A.V., 2019. Suspended-Matter Distribution near the Western Coast of Crimea under the Impact of Strong Winds of Various Directions. *Izvestiya, Atmospheric and Oceanic Physics*, 55(9), pp. 1138-1149. doi:10.1134/s0001433819090044

9. Mahadevan, A., 2016. The Impact of Submesoscale Physics on Primary Productivity of Plankton. *Annual Review of Marine Science*, 8, pp. 161-184. doi:10.1146/annurev-marine-010814-015912

10. Mezić, I., Loire, S., Fonoberov, V.A. and Hogan, P., 2010. A New Mixing Diagnostic and Gulf Oil Spill Movement. *Science*, 330(6003), pp. 486-489. doi:10.1126/science.1194607

11. Rascle, N., Molemaker, J., Marié, L., Nouguier, F., Chapron, B., Lund, B. and Mouche, A., 2017. Intense Deformation Field at Oceanic Front Inferred from Directional Sea Surface Roughness Observations. *Geophysical Research Letters*, 44(11), pp. 5599-5608. doi:10.1002/2017GL073473

12. Kudryavtsev, V., Akimov, D., Johannessen, J.A. and Chapron, B., 2005. On Radar Imaging of Current Features: 1. Model and Comparison with Observations. *Journal of Geophysical Research: Oceans*, 110(C7), C07016. doi:10.1029/2004JC002505

13. Kudryavtsev, V., Myasoedov, A., Chapron, B., Johannessen, J.A. and Collard, F., 2012. Imaging Mesoscale Upper Ocean Dynamics Using Synthetic Aperture Radar and Optical Data. *Journal of Geophysical Research: Oceans*, 117(C4), C04029. doi:10.1029/2011JC007492

14. Garrett, C.J.R. and Loder, J.W., 1981. Dynamical Aspects of Shallow Sea Fronts. *Philosophical Transactions of the Royal Society of London. Series A, Mathematical and Physical Sciences*, 302(1472), pp. 563-581. doi:10.1098/rsta.1981.0183

15. Klein, P. and Hua, B.L., 1990. The Mesoscale Variability of the Sea Surface Temperature: An Analytical and Numerical Model. *Journal of Marine Research*, 48(4), pp. 729-763. doi:10.1357/002224090784988700

16. Garrett, C., 1976. Generation of Langmuir Circulations by Surface Waves – A Feedback Mechanism. *Journal of Marine Research*, 34(1), pp. 117-130.

17. Resseguier, V., Mémin, E. and Chapron, B., 2017. Geophysical Flows under Location Uncertainty, Part III: SQG and Frontal Dynamics under Strong Turbulence Conditions. *Geophysical & Astrophysical Fluid Dynamics*, 111(3), pp. 209-227. doi:10.1080/03091929.2017.1312102

18. Isern-Fontanet, J., Chapron, B., Lapeyre, G. and Klein, P., 2006. Potential Use of Microwave Sea Surface Temperatures for the Estimation of Ocean Currents. *Geophysical Research Letters*, 33(24), L24608. doi:10.1029/2006GL027801

19. Isern-Fontanet, J., Lapeyre, G., Klein, P., Chapron, B. and Hecht, M.W., 2008. Three-Dimensional Reconstruction of Oceanic Mesoscale Currents from Surface Information. *Journal of Geophysical Research: Oceans*, 113(C9), C09005. doi:10.1029/2007JC004692

20. Giordani, H., Caniaux, G., Prieur, L., Paci, A. and Giraud, S., 2005. A 1 Year Mesoscale Simulation of the Northeast Atlantic: Mixed Layer Heat and Mass Budgets during the POMME Experiment. *Journal of Geophysical Research: Oceans*, 110(C7), C07S08. https://doi.org/10.1029/2004JC002765

21. Nagai, T., Tandon, A. and Rudnick, D.L., 2006. Two-Dimensional Ageostrophic Secondary Circulation at Ocean Fronts due to Vertical Mixing and Large-Scale Deformation. *Journal of Geophysical Research: Oceans*, 111(C9), C09038. doi:10.1029/2005JC002964

22. Ponte, A., Klein, P., Capet, X., Le Traon, P.Y., Chapron, B. and Lherminier, P., 2013. Diagnosing Surface Mixed Layer Dynamics from High-Resolution Satellite Observations: Numerical Insights. *Journal of Physical Oceanography*, 43(7), pp. 1345-1355. doi:10.1175/jpo-d-12-0136.1

23. Cronin, M.F. and Kessler, W.S., 2009. Near-Surface Shear Flow in the Tropical Pacific Cold Tongue Front. *Journal of Physical Oceanography*, 39(5), pp. 1200-1215. doi:10.1175/2008jpo4064.1

24. Crowe, M.N. and Taylor, J.R., 2020. The Effects of Surface Wind Stress and Buoyancy Flux on the Evolution of a Front in a Turbulent Thermal Wind Balance. *Fluids*, 5(2), 87. https://doi.org/10.3390/fluids5020087

25. Wenegrat, J.O. and McPhaden, M.J., 2016. Wind, Waves, and Fronts: Frictional Effects in a Generalized Ekman Model. *Journal of Physical Oceanography*, 46(2), pp. 371-394. doi:10.1175/jpo-d-15-0162.1

26. Sheres, D., Kenyon, K.E., Bernstein, R.L. and Beardsley, R.C., 1985. Large Horizontal Surface Velocity Shears in the Ocean Obtained from Images of Refracting Swell and In Situ Moored Current Data. *Journal of Geophysical Research: Oceans*, 90(C3), 4943. https://doi.org/10.1029/jc090ic03p04943

27. Grodsky, S., Kudryavtsev, V. and Ivanov, A., 2000. Quasisynchronous Observations of the Gulf Stream Frontal Zone with Almaz-1 SAR and Measurements Taken on Board the R/V Akademik Vernadsky. *The Global Atmosphere and Ocean System*, 7, pp. 249-272.

28. Kudryavtsev, V., Yurovskaya, M., Chapron, B., Collard, F. and Donlon, C., 2017. Sun Glitter Imagery of Surface Waves. Part 2: Waves Transformation on Ocean Currents. *Journal of Geophysical Research: Oceans*, 122(2), pp. 1384-1399. doi:10.1002/2016JC012426

29. Dulov, V.A. and Kudryavtsev, V.N., 1990. Imagery of the Inhomogeneities of Currents on the Ocean Surface State. *Soviet Journal of Physical Oceanography*, 1(5), pp. 325-336. doi:10.1007/BF02196830

30. Lyzenga, D.R., 1998. Effects of Intermediate-Scale Waves on Radar Signatures of Ocean Fronts and Internal Waves. *Journal of Geophysical Research: Oceans*, 103(C9), pp. 18759-18768. doi:10.1029/98jc01189

31. Kubryakov, A.A., Kudryavtsev, V.N. and Stanichny, S.V., 2021. Application of Landsat Imagery for the Investigation of Wave Breaking. *Remote Sensing of Environment*, 253, 112144. https://doi.org/10.1016/j.rse.2020.112144

32. Phillips, O.M., 1984. On the Response of Short Ocean Wave Components at a Fixed Wavenumber to Ocean Current Variations. *Journal of Physical Oceanography*, 14(9), pp. 1425-1433. https://doi.org/10.1175/1520-0485(1984)014<1425:OTROSO>2.0.CO;2

33. Brannigan, L., Marshall, D.P., Naveira Garabato, A.C., Nurser, A.G. and Kaiser, J., 2017. Submesoscale Instabilities in Mesoscale Eddies. *Journal of Physical Oceanography*, 47(12), pp. 3061-3085. https://doi.org/10.1175/JPO-D-16-0178.1

34. Zatsepin, A., Kubryakov, A., Aleskerova, A., Elkin, D. and Kukleva, O., 2019. Physical Mechanisms of Submesoscale Eddies Generation: Evidences from Laboratory Modeling and Satellite Data in the Black Sea. *Ocean Dynamics*, 69(2), pp. 253-266. https://doi.org/10.1007/s10236-018-1239-4

35. Kilic, L., Prigent, C., Aires, F., Boutin, J., Heygster, G., Tonboe, R.T., Roquet, H., Jimenez, C. and Donlon, C., 2018. Expected Performances of the Copernicus Imaging Microwave Radiometer (CIMR) for an All-Weather and High Spatial Resolution Estimation of Ocean and Sea Ice Parameters. *Journal of Geophysical Research: Oceans*, 123(10), pp. 7564-7580. doi:10.1029/2018JC014408

36. Morrow, R., Fu, L.-L., Ardhuin, F., Benkiran, M., Chapron, B., Cosme, E., d'Ovidio, F., Farrar, J.T., Gille, S.T. [et al.], 2019. Global Observations of Fine-Scale Ocean Surface Topography with the Surface Water and Ocean Topography (SWOT) Mission. *Frontiers in Marine Science*, 6, 232. doi:10.3389/fmars.2019.00232

37. Lumpkin, R., Özgökmen, T. and Centurioni, L., 2017. Advances in the Application of Surface Drifters. *Annual Review of Marine Science*, 9, pp. 59-81. https://doi.org/10.1146/annurev-marine-010816-060641

38. Rascle, N., Nouguier, F., Chapron, B. and Ocampo-Torres, F.J., 2018. Sunglint Images of Current Gradients at High Resolution: Critical Angle and Directional Observing Strategy. *Remote Sensing of Environment*, 216, pp. 786-797. https://doi.org/10.1016/j.rse.2018.06.011

39. Kudryavtsev, V.N., Chapron, B., Myasoedov, A.G., Collard, F. and Johannessen, J.A., 2013. On Dual Co-Polarized SAR Measurements of the Ocean Surface. *IEEE Geoscience and Remote Sensing Letters*, 10(4), pp. 761-765. doi:10.1109/LGRS.2012.2222341

40. Kudryavtsev, V., Kozlov, I., Chapron, B. and Johannessen, J., 2014. Quad-Polarization SAR Features of Ocean Currents. *Journal of Geophysical Research: Oceans*, 119(9), pp. 6046-6065. https://doi.org/10.1002/2014JC010173

41. Chapron, B., Collard, F. and Ardhuin, F., 2005. Direct Measurements of Ocean Surface Velocity from Space: Interpretation and Validation. *Journal of Geophysical Research: Oceans*, 110(C7), C07008. doi:10.1029/2004JC002809

42. Gommenginger, C., Chapron, B., Hogg, A., Buckingham, C., Fox-Kemper, B., Eriksson, L., Soulat, F., Ubelmann, C., Ocampo-Torres, F. [et al.], 2019. SEASTAR: A Mission to Study Ocean Submesoscale Dynamics and Small-Scale Atmosphere-Ocean Processes in Coastal, Shelf and Polar Seas. *Frontiers in Marine Science*, 6, 457. doi:10.3389/fmars.2019.00457

About the authors:

Bertrand Chapron, the Head of the Spatial Oceanography Group, Institut Français de Recherche Pour l'exploitation de la MER (IFREMER, Centre Bretagne, ZI de la Pointe du Diable, CS 10070, 29280 Plouzané, France), scientific leader of the Satellite Oceanography Laboratory at Russian State Hydrometeorological University (79 Voronezhskaya St., St. Petersburg, 192007, Russian Federation), **Scopus Author ID: 56209544000**, bertrand.chapron@ifremer.fr

Vladimir N. Kudryavtsev, leading Research Associate, FSBSI FRC MHI (2 Kaptanskaya St., Sevastopol, Russian Federation, 299011), the Head of the Satellite Oceanography Laboratory, Russian State Hydrometeorological University (79 Voronezhskaya St., St. Petersburg, 192007, Russian Federation), Dr. Sci. (Maths.-Phys.), **Scopus Author ID: 7102703183**, kudr@rshu.ru

Fabrice Collard, the President of OceanDataLab (870, Route de Deolen - 29280 Locmaria Plouzané, France), **Scopus Author ID 36980751900**, dr.fab@oceandatalab.com

Nicolas Rascle, Researcher Centro de Investigación Científica y de Educación Superior de Ensenada (Baja California, México), **Scopus Author ID: 23006078500**, nrascle@cicese.mx

Arseniy A. Kubryakov, Senior Research Associate, Remote Sensing Department, Marine Hydrophysical Institute of RAS (2 Kaptanskaya St., Sevastopol, Russian Federation, 299011), Ph. D (Maths.-Phys.), **ORCID ID: 0000-0003-3561-5913**, arskubr@mhiras.ru

Sergey V. Stanichny, Senior Research Associate, the Head of Remote Sensing Department, Marine Hydrophysical Institute of RAS (2 Kaptanskaya St., Sevastopol, Russian Federation, 299011), Ph. D (Math.-Phys.), **ORCID ID: 0000-0002-1033-5678**, stanichny@mhi-ras.ru

Contribution of the co-authors:

Bertrand Chapron – conceptualization, writing – original draft preparation, investigation, methodology
Vladimir N. Kudryavtsev – conceptualization, project administration, writing – review and editing
Fabrice Collard – investigation, visualization, data curation, formal analysis
Nicolas Rascle – visualization, formal analysis
Arseniy A. Kubryakov – writing – review and editing
Sergey V. Stanichny – investigation

All the authors have read and approved the final manuscript.
The authors declare that they have no conflict of interest.